Hindawi
Advances in Civil Engineering
Volume 2018, Article ID 9784360, 11 pages
https://doi.org/10.1155/2018/9784360

*Research Article*

# Computational Study of Cold-Formed-Steel X-Braced Shear Walls

**Metwally Abu-Hamd, Maheeb Abdel-Ghaffar, and Basel El-Samman**

*Structural Engineering Department, Faculty of Engineering, Cairo University, Giza, Egypt*

Correspondence should be addressed to Basel El-Samman; basel.elsamman@gmail.com

Received 21 October 2017; Revised 13 January 2018; Accepted 29 January 2018; Published 19 March 2018

Academic Editor: Giovanni Garcea



The aim of this paper was to present a verified finite element method that represents the full-scale-braced shear walls under seismic loads and to study their ductility. The models account for different types of material and geometric nonlinearities. The screws that connect the cold-formed-steel (CFS) studs, tracks, gusset plates, and braces are considered explicitly in the model. The deformation of the hold-downs under the horizontal load is considered. The finite element program ANSYS (2012) is used to model and analyze the case studies. A parametric study is performed to investigate the response modification factor ($R$) of the CFS-braced shear walls. The parametric study showed that the North American Specification is about 20% conservative in estimating the ($R$) factor.

## 1. Introduction

A noteworthy increase has occurred in the use of the light gauge cold-formed-steel framing in the residential buildings in the last few decades. In Egypt, cold-formed-steel is generally used in the industrial buildings as roof purlins and side girts. Recently, with the spread of the usage of the CFS in residential buildings, some buildings are constructed with CFS in Egypt like the Digital Library in Cairo University. International specifications like Canadian and North American specification concentrated on the use of CFS-braced shear walls depending on several researches. These specifications are studied in this research. The use of cold-formed-steel has many advantages such as durability, lightweight, recyclability, and rapid construction. These advantages are essential reasons for this growth in CFS construction.

A CFS strap-braced shear wall consists of vertical studs collected by top and bottom tracks. Diagonal strap braces are added to give the wall lateral stability. All these elements are connected with screws or welds. The shear wall components are designed to transfer the lateral earthquake load to the foundations. The diagonal strap brace was detailed to develop plastic deformations that would dissipate earthquake energy and allow ductile behavior.

Uang [1] derived the basic formulas for establishing the response modification factor $R$ and the displacement amplification factor Cd used in the National Earthquake Hazards Reduction Program (NEHRP) recommended provisions. These terms are primarily functions of both the structural overstrength and structural ductility factors. These factors could be concluded from monotonic inelastic limit load analysis and widely used by researchers to investigate the reduction factor $R$.

Al-Kharat and Rogers [2–4] performed several full-scale tests on CFS strap-braced shear walls with different aspect ratios. Monotonic- and cyclic-braced walls tests showed that when the capacity design requirements were used, a ductile behavior was reached. This was achieved by designing the strap braces as a fuse member while designing other wall elements to sustain the expected brace capacity. Those experimental results are computationally verified in this study.

Casafont et al. [5] made an experiment on the screwed connection of the strap. They found that the Eurocode formulas give good estimation for the connection failure.

Hatami et al. [6] conducted laboratory tests on 2.4 m × 2.4 m CFS shear walls with perforated straps. They found that the brittle failure mode of net section fracture at connection screw holes locations disappeared when the perforated straps are used which resulted in ductile behavior.

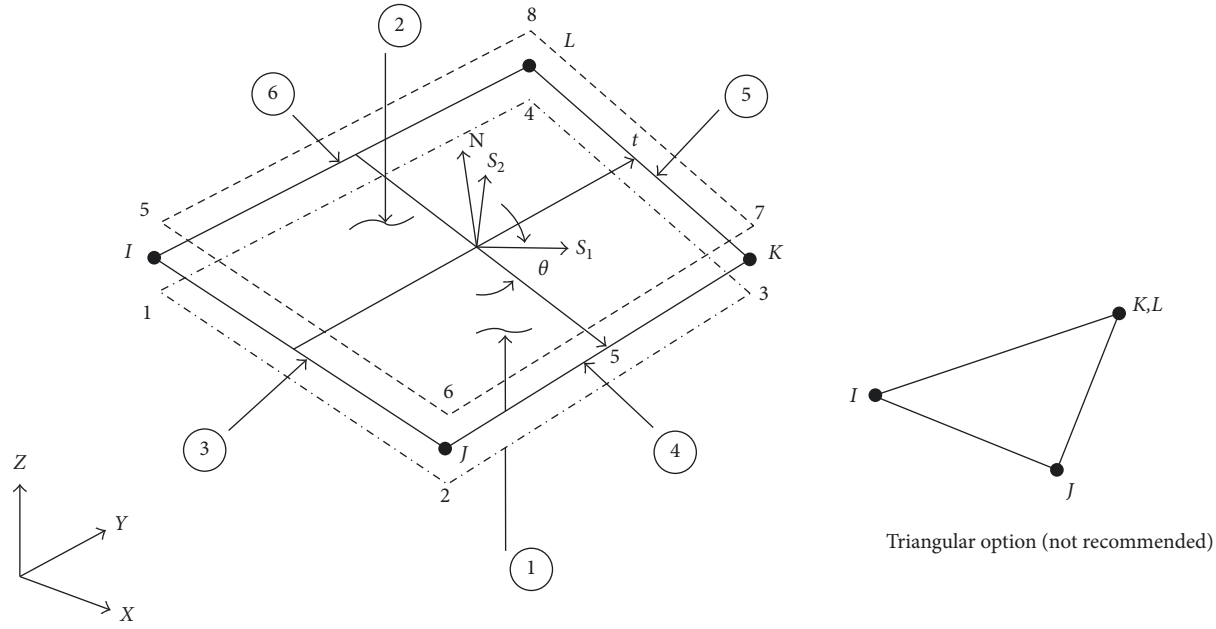


Figure 1: SHELL181 formulation.

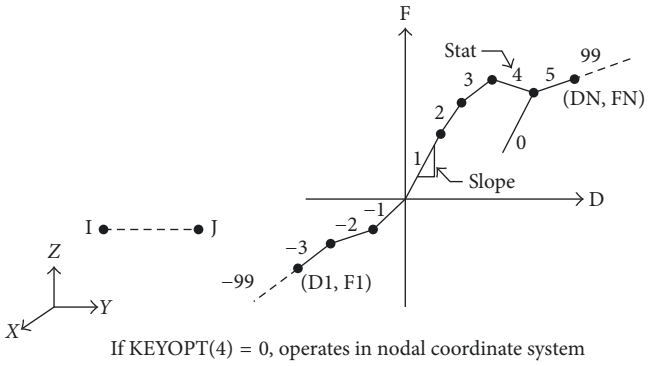


Figure 2: COMBIN39 formulation.

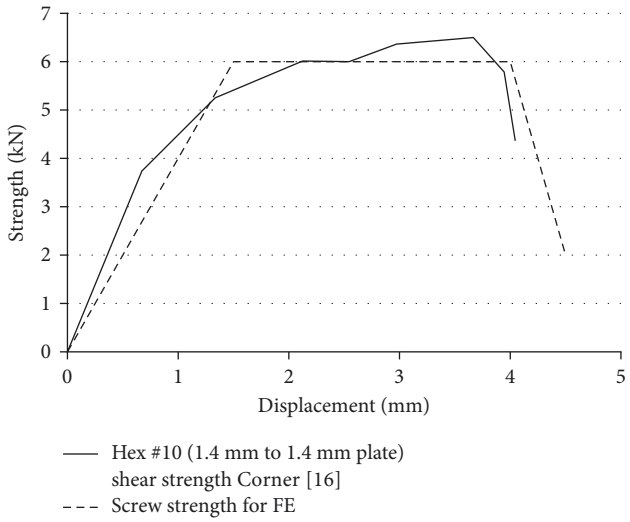


Figure 3: Screw strength.

Velchev et al. [7] evaluated typical weld- and screw-connected single-story strap-braced walls with respect to their ability to resist lateral in-plane loads in the inelastic range. The results were used to verify the new strap-braced wall seismic design provisions in AISI S213 [8]. A total of 44 tension-only X-braced walls with aspect ratios from 4 : 1 to 1 : 1 were tested under lateral loading using monotonic and reversed cyclic protocols. *R* factors were calculated based on the measured ductility and overstrength of the test walls and compared with the values recommended by AISI S213 [8].

Mahmoudi and Abdi [9] evaluated overstrength, ductility, and response modification factors in special moment-resisting frames with TADAS (triangular-plate added damping and stiffness) devices. The *R*-factor for special moment-resisting frames with and without TADAS devices has been determined separately.

Abu-Hamd and El-Samman [10] investigated the buckling strength of the built-up cold-formed I-sections made of two CFS back-to-back C-sections. These columns are generally used as chord studs in CFS-braced shear walls.

Landolfo et al. [11] performed laboratory tests for twelve full-scale X-braced shear walls of dimensions 2.4 m (width) × 2.7 m (height) under monotonic and cyclic loading. They concluded that when the capacity design criteria are performed, the undesirable brittle failures of connections, tracks, studs, and anchorages did not occur. Those monotonic test results are also computationally verified in this study.

## 2. Methodology and Scope of Work

Two main objectives are targeted in this research to perform nonlinear verification analysis for CFS-braced shear walls that were previously tested by other researchers and to perform parametric study using the nonlinear FE model that is already verified and thus investigate the response reduction factor *R*.

Table 1: Al-Kharat's CFS walls elements dimensions.

| Specimen | Chord studs | Intermediate studs | Tracks | Braces |
|---|---|---|---|---|
| 9C-M | 152.4 × 41.3 × 12.7 × 1.37 | 152.4 × 41.3 × 12.7 × 1.09 | 152.4 × 31.8 × 1.37 | 127 × 1.09 |
| 39-M | 152.4 × 41.3 × 12.7 × 1.37 | 152.4 × 41.3 × 12.7 × 1.09 | 152.4 × 31.8 × 1.37 | 69.8 × 1.37 |
| 45-M | 152.4 × 41.3 × 12.7 × 1.73 | 152.4 × 41.3 × 12.7 × 1.09 | 152.4 × 31.8 × 1.73 | 101.6 × 1.73 |

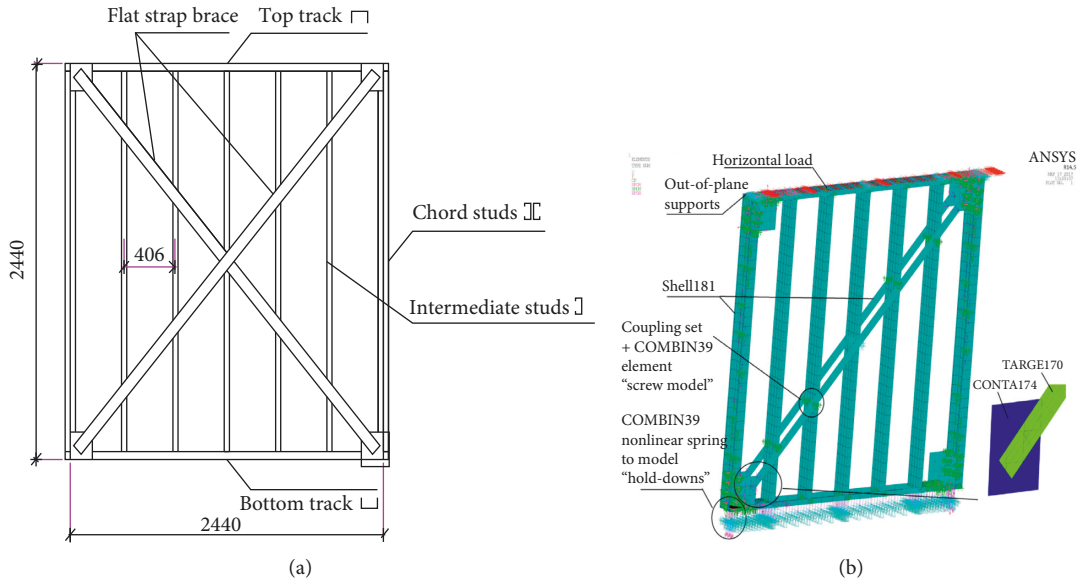


Figure 4: Wall setup (Al-Kharat).

Table 2: Material yield stress (MPa).

| Specimen | Chord studs | | Intermediate studs | | Tracks | | Braces | |
|---|---|---|---|---|---|---|---|---|
| | $F_{yn}$ (MPa) | $F_{y,exp}$ (MPa) | $F_{yn}$ (MPa) | $F_{y,exp}$ (MPa) | $F_{yn}$ (MPa) | $F_{y,exp}$ (MPa) | $F_{yn}$ (MPa) | $F_{y,exp}$ (MPa) |
| 9C-M | 340 | 383 | 230 | 290 | 340 | 388 | 230 | 290 |
| 39-M | 340 | 383 | 230 | 290 | 340 | 388 | 340 | 396 |
| 45-M | 340 | 383 | 230 | 290 | 340 | 388 | 340 | 365 |

*2.1. Finite Element Model.* This model should investigate four main parameters: (1) the CFS shear wall behavior within the elastic range, (2) the wall strength at yielding, (3) the wall ultimate strength, and (4) the reason of failure. All parameters are compared with test results, namely, six verification specimens that were tested by Al-Kharat and Rogers [4] and by Landolfo et al. [11].

Using the program ANSYS, verification case studies are considered to insure the accuracy of our model. The main finite element used in the model is SHELL181 for the studs, tracks, gusset plates, hold-downs, and braces. SHELL181 is suitable for analyzing thin shell structures and is widely used to model CFS. This element has good convergence and accounts for both geometric and material nonlinearities. This element is shown in Figure 1 and described in details in the manual of ANSYS [12].

The screws connecting the studs were modeled using "coupling set" in the out-of-plane while the shear nonlinear failure in-plane mode of the screws is modeled using two nonlinear spring elements COMBIN39. COMBIN39 is a unidirectional element with nonlinear generalized force-deflection capability that can be used in any analysis. The element has longitudinal or torsional capability in 1-D, 2-D, or 3-D applications. The longitudinal option is a uniaxial tension-compression element with up to three degrees of freedom at each node: translations in the nodal $x$, $y$, and $z$ directions. No bending or torsion is considered. The force-deflection curve should be input such that deflections are increasing from the third (compression) to the first (tension) quadrants. If the force-deflection curve is exceeded, the last defined slope is maintained. The element input is shown in Figure 2, and more details are given in the manual of ANSYS [12].

The displacement occurs at the hold-downs, and the floor below the wall is also modeled using nonlinear spring COMBIN39 with different real constants input to be similar to that concluded by Buonopane et al. [13]. Contact elements surface to surface (TARGE170 and CONTA174) are used to model the connections between the bracing and the gusset plate. Details about both elements are described in the manual of ANSYS [12].

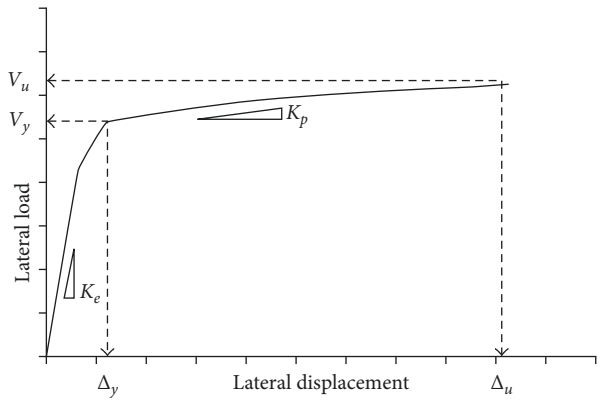


Figure 5: Main parameters of load deflection curve.

Table 3: Results summary.

| | Finite element | | | | | | Test results | | | | FE/test results (dev. %) | | | |
|---|---|---|---|---|---|---|---|---|---|---|---|---|---|---|
| | $V_u$ (kN) | $V_y$ (kN) | $\Delta_u$ (mm) | $\Delta_y$ (mm) | $K_e$ kN/mm | $K_p$ kN/mm | $V_u$ (kN) | $V_y$ (kN) | $\Delta_u$ (mm) | $\Delta_y$ (mm) | $V_u$ | $V_y$ | $\Delta_u$ | $\Delta_y$ |
| 9C | 64 | 59 | 100 | 20 | 2.95 | 0.06 | 60 | 56 | 110 | 18 | 7% | 5% | 9% | 11% |
| 39A | 62 | 54 | 185 | 22 | 2.45 | 0.05 | 67 | 53 | 200 | 26 | 7% | 2% | 8% | 15% |
| 45A | 103 | 92 | 165 | 26 | 3.54 | 0.08 | 107 | 93 | 180 | 28 | 4% | 1% | 8% | 7% |

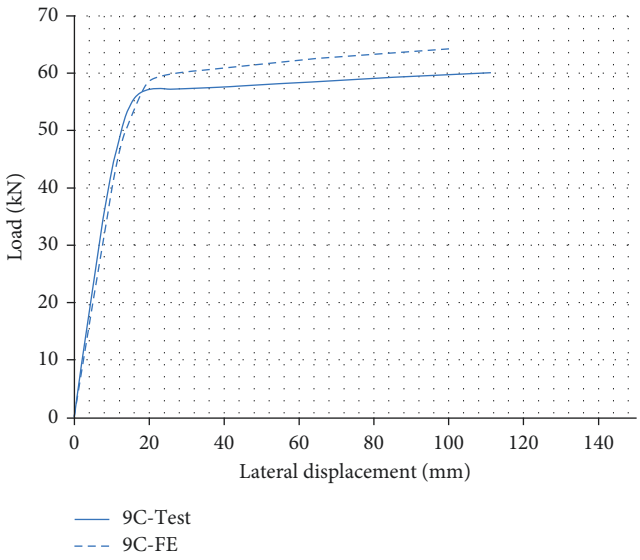


Figure 6: Load-deflection verification curve of test versus FE (specimen 9C).

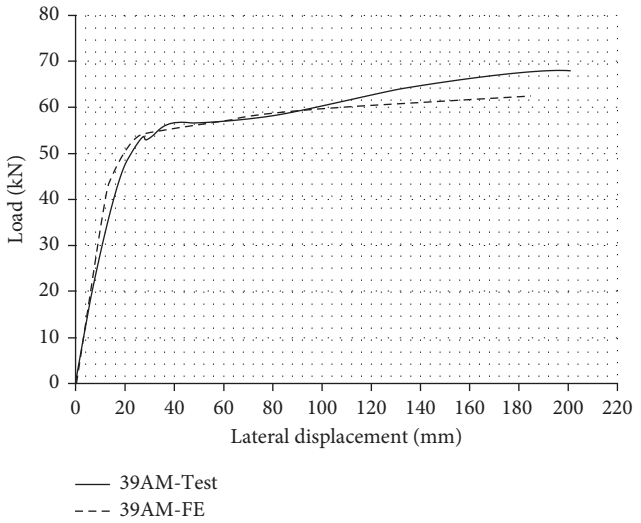


Figure 7: Load-deflection verification curve of test versus FE (specimen 39AM).

At first, both compression and tension braces were modeled and then compared to tension bracing only. Much time in the analysis was clearly saved while having similar results. Therefore, only the tension diagonal brace is considered in FEM to simplify the analysis as it is used only for monotonic loading.

*2.1.1. Modeling of Boundary Conditions (Out-of-Plane Support).* As done in experiments, a horizontal out-of-plane roller support is assigned at each top track node to prevent the movement out of plane but allow the movement vertically and horizontally in-plane.

*2.2. Modeling of Hold-Downs and Anchor Bolts.* From previous tests, there is a portion of the displacement that occurred due to the vertical displacement of the hold-down under the tension reaction. The reference nodes defining the hold-down elements are connected to nodes on the ground in the vertical direction via a bilinear spring. This modeling

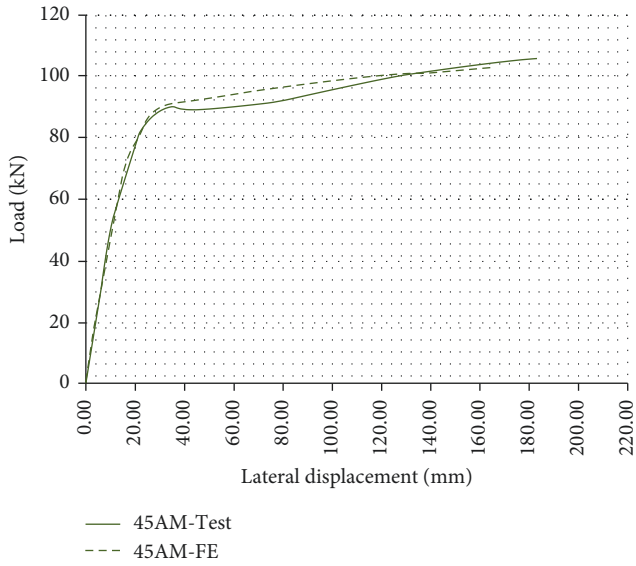


Figure 8: Load-deflection verification curve of test versus FE (specimen 45AM).

Table 4: Landolfo's CFS walls elements dimensions.

| Specimen | Chord studs | Intermediate studs | Tracks | Braces | Steel grade |
|---|---|---|---|---|---|
| WLE | $150 \times 50 \times 20 \times 1.5$ | $150 \times 50 \times 20 \times 1.5$ | $153 \times 50 \times 1.5$ | $90 \times 1.5$ | S350 |
| WLD | $150 \times 50 \times 20 \times 1.5$ | $150 \times 50 \times 20 \times 1.5$ | $153 \times 50 \times 1.5$ | $70 \times 2$ | S235 |
| WHD | $150 \times 50 \times 20 \times 3$ | $150 \times 50 \times 20 \times 3$ | $153 \times 50 \times 1.5$ | $140 \times 2$ | S235 |

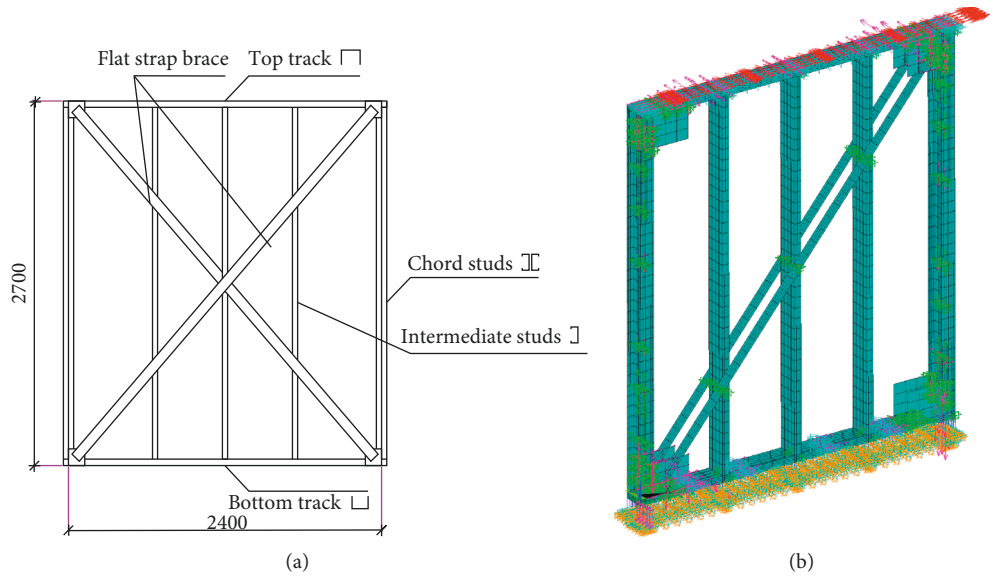


Figure 9: Wall setup (Landolfo).

choice is based on the study of Buonopane et al. [13] in which modeling the tension flexibility of the hold-down is established. Herein, the tension stiffness of the hold-down is selected to be 10 kN/mm based on Leng et al. [14]. The compression stiffness is chosen to be thousand times of the tension stiffness based on the assumption that axial force in chord studs is transferred by bearing to the foundation when the hold-down is in compression. The bilinear spring connecting the reference node to a node on the ground is modeled by means of nonlinear spring element type COMBIN39 in ANSYS.

*2.3. Connection between Gusset Plates and Braces.* Due to the mismatch between the mesh arrangement of the gusset

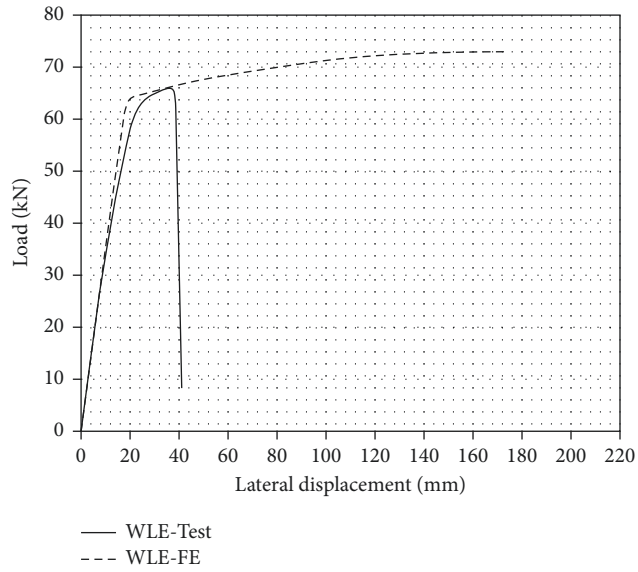


Figure 10: Load-deflection verification curve of test versus FE (specimen WLE).

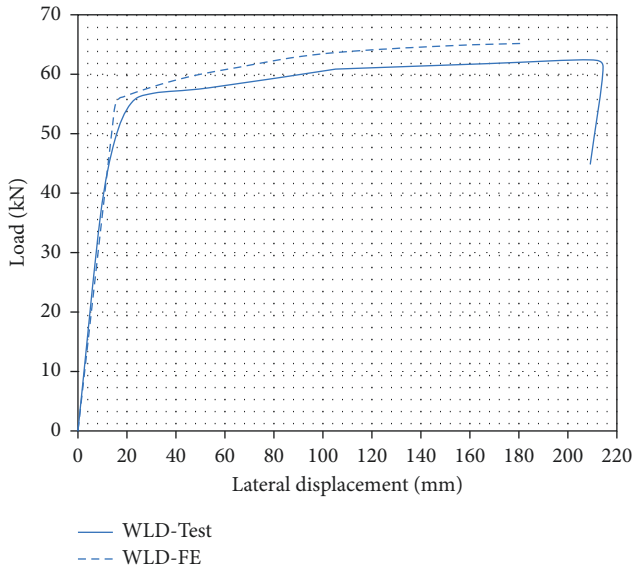


Figure 11: Load-deflection verification curve of test versus FE (specimen WLD).

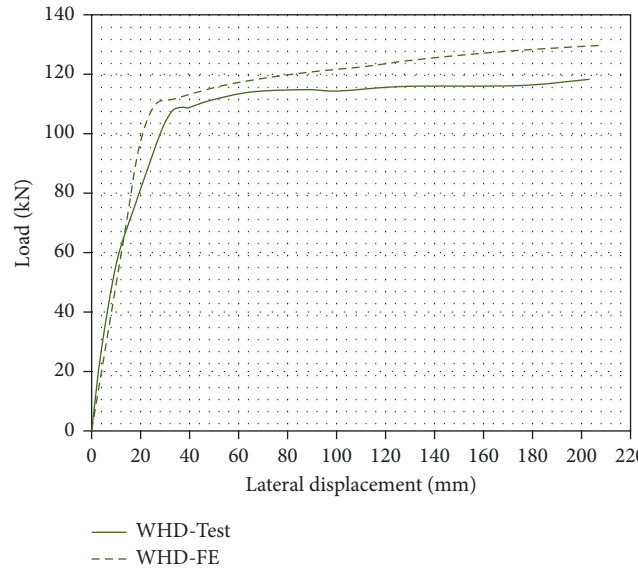


Figure 12: Load-deflection verification curve of test versus FE (specimen WHD).

plates and the braces as a result of the inclination of the braces, it was decided to do the assembly by using contact element provided in ANSYS. This simulation is good enough because connections are always overdesigned, and failure will occur outside the connection, in the brace itself.

*2.4. Screws Connection: Nonlinear Behavior.* As mentioned before, the screws connecting the studs modeled using "coupling set" in the out-of-plane while the shear nonlinear failure in-plane mode of the screws is modeled using two nonlinear spring elements COMBIN39. Serrette and Peyton [15] reviewed the design provisions for screw-fastened cold-formed-steel connections in the United States. In addition, they examined the relationship between the connected elements, computed connection strength, and the strength of the connector. They also prepared fastener-strength tables for the three manufacturers based on testing. Corner [16] predicted the tilting angle and the limit states of single-fastened cold-formed steel-to-steel shear connection. According to the steel plate thicknesses studied in this research, the screw strength is modeled as shown in Figure 3.

*2.5. Nonlinear Analysis Steps.* In order to consider the geometrical and material nonlinear behavior in such cases, two types of analyses are considered. The first is an eigen buckling analysis that predicts the buckling modes and

Table 5: Results summary.

| | Finite element | | | | | | Test results | | | | FE/test results (dev. %) | | | |
|---|---|---|---|---|---|---|---|---|---|---|---|---|---|---|
| | $V_u$ (kN) | $V_y$ (kN) | $\Delta_u$ (mm) | $\Delta_y$ (mm) | $K_e$ kN/mm | $K_p$ kN/mm | $V_u$ (kN) | $V_y$ (kN) | $\Delta_u$ (mm) | $\Delta_y$ (mm) | $V_u$ | $V_y$ | $\Delta_u$ | $\Delta_y$ |
| WLE | 73 | 64 | 170 | 18 | 3.56 | 0.06 | 66 | 63 | * | 20 | 11% | 2% | * | 10% |
| WLD | 65 | 56 | 182 | 17 | 3.29 | 0.05 | 62 | 56 | 210 | 20 | 5% | 0% | 13% | 15% |
| WHD | 130 | 112 | 200 | 26 | 4.31 | 0.10 | 119 | 108 | 200 | 30 | 9% | 4% | 0% | 13% |

*Specimen failed due to connection failure after reaching the yielding limit. Connection failure is excluded in the FE model.

buckling frequencies. In this problem, the material behavior is assumed to be elastic, and the member is considered to have perfect geometry. The lowest buckling modes predicted from the eigen buckling analysis are subsequently used to model the geometric imperfections. To model the overall imperfections, typically L/1000 is used as the magnitude while the first global buckling mode shape is used for the distribution shape. On the other hand, local buckling magnitude is considered as half of the wall thickness according to Zeinoddini and Schafer [17] and using the first local buckling mode shape.

The second type of analysis is a nonlinear load-displacement analysis of the real wall structures under the action of applied loads in the presence of initial geometrical imperfections and material nonlinearity. The ultimate strength and failure modes are determined from this analysis when they reach the limit point located on its equilibrium path. At this limit point, the corresponding load parameter value and deformed configuration provide the wall ultimate strength and failure mode.

## 3. Description of Al-Kharat's Case Studies

Three square specimens were tested with dimensions $2.44 \times 2.44$ m. Each specimen consists of 2 chord studs of built-up I-shaped CFS C-shaped studs. Five vertical intermediate C-shaped studs were spaced at 406 mm. All studs were collected using top and bottom U-shaped tracks using hex-washer-head self-drilling screws. X-braces were connected to tracks and chord studs using screwed gusset plates. The dimensions and materials of all elements differ from one specimen to another as shown in Table 1 and Figure 4 (in mms).

*3.1. Material Model.* The material is modeled in ANSYS [12] as a linear isotropic material in the elastic range with elastic modulus 205 kN/mm$^2$ and Poisson's ratio 0.3. In the inelastic range, the material is defined to be bilinear isotropic with nominal yield stress from coupon tests according to Al-Karat and Rogers [4], as shown in Table 2.

*3.2. Specimens FE Results Discussion.* In all the case studies, the reason of failure is the yielding of the brace material which is similar to the tests. The chord stud that is under compression has a buckling deformation that results in the decrease of the wall strength gradually which leads to excessive strains and failure. The existence of the stiffening parts in the top and bottom tracks is very important to exclude the possibility of having local failure. It is clear that the intermediate studs do not participate in the lateral shear wall strength; however, they have another important role to work as lateral support points at the point of connection with the bottom and top tracks. Besides that the gusset plates connect the braces straps to the shear wall, it also gives the connection between the chord studs and the tracks some rigidity.

Table 6: Landolfo's CFS walls coupon test results.

| Specimen type | Thickness (mm) | $F_{yn}$ (Mpa) | $F_{y,exp}$ (Mpa) |
|---|---|---|---|
| S235-2 | 2 | 235 | 302 |
| S350-1.5 | 1.5 | 350 | 355 |
| S350-3 | 3 | 350 | 364 |

Figure 5 indicates the main parameters that were investigated in verification case studies. $V_u$ and $V_y$ define the ultimate strength and the maximum elastic strength, respectively. $\Delta_u$ and $\Delta_y$ define the ultimate displacement and the maximum elastic displacement, respectively. $K_p$ and $K_e$ define the wall plastic stiffness and the wall elastic stiffness, respectively. All previous parameters resulting from FE simulation model were compared with similar parameters from experiment. The FE shows very accurate results compared with experimental results. Table 3 shows the FE results and the comparison with the experimental results. According to Table 3, The FE model can predict the wall strength with an average accuracy error of 4% and the wall lateral displacement with an average accuracy error of 10%. These results ensure that the developed FE model is reliable to simulate the inelastic behavior of the CFS shear walls and to be used in the parametric study. Figures 6–8 show the shear wall results and the load-deflection curves of different specimens. It is clear that all test specimens failed due to strap brace yield which indicates that all specimen components other than the braces were already overdesigned to guarantee that the strap brace achieve a plastic behavior. The FE was modeled to ensure that the failure will occur at the braces which are similar to what occurred at the test.

## 4. Description of Landolfo's Case Studies

Three typical wall configurations were defined according to both elastic and dissipative design criteria for three different seismic scenarios. The lateral in-plane inelastic behavior of these systems was evaluated by twelve tests performed on full-scale Cold-formed strap-braced stud wall specimens with dimensions $2400 \times 2700$ m subjected to monotonic loading. In our verification study, monotonic loading only is studied

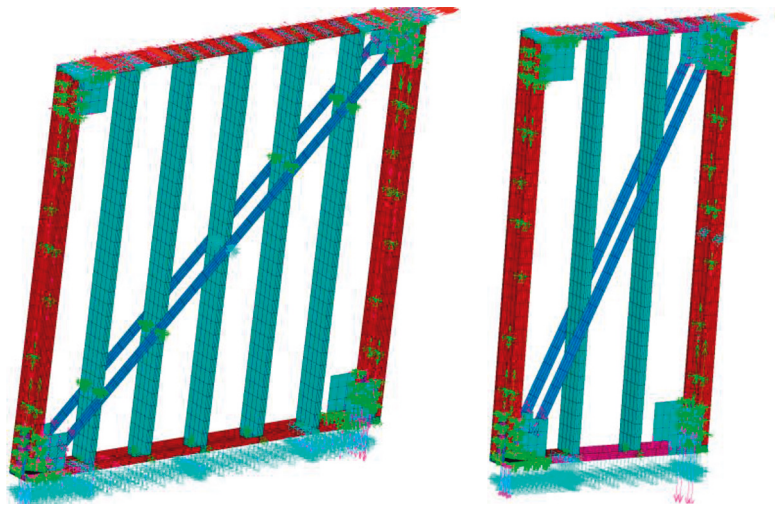

(a) (b)

Figure 13: (a) Wall with aspect ratio 1 : 1 model. (b) Aspect ratio 1 : 2 model.

for the three wall configurations which are defined as follows: elastic light (WLE), dissipative light (WLD), and dissipative heavy (WHD) walls. The dimensions of the three walls are listed in Table 4. Wall configuration is shown in Figure 9.

The lateral response of these systems was investigated by testing each of the three selected configurations by monotonic loading on full-scale wall specimens in size of $2400 \times 2700$ mm. Figures 10–12 show the shear wall results and the load-deflection curves of different specimens. From tests results, walls specimens WHE and WHD failed due to strap brace yield which is similar to the FE mode behavior. Specimen WLE failed due to net section fracture at the screws which is not considered in the FE model. In WLE specimen, the elastic range only is considered in the comparison. Table 5 shows the verification results.

*4.1. Material Model.* The material is modeled in ANSYS [12] as linear isotropic material in the elastic range with elastic modulus 205 kN/mm$^2$ and Poisson's ratio 0.3. In the inelastic range, the material is defined to be bilinear isotropic with nominal yield stress from coupon tests according to Landolfo et al. [11], as shown in Table 6.

## 5. Parametric Study for the Response Modification Factor

Different codes use certain factor to reduce seismic forces on structures because structures can dissipate the same energy from earthquake with lower loads but more displacements depending on the overall structural ductility.

The American Society of Civil Engineers ASCE/SEI 7-10 Standard [18] agrees to an $R$ factor of 3.25 to be considered in the design of ordinary concentrically braced CFS frames.

The $R$ factor can be increased to 4 if the capacity design approach is considered according to AISI S213 [8]. The value of 4 of the $R$ factor is also used by the US Army Corps of Engineers TI 809-07 Technical Instructions [19] which are used in the design of CFS systems. It also recommends that a capacity design approach should be followed.

In the National Building Code of Canada NBCC [20], $R$ is called the force reduction factor which is defined by two factors $R_d$ and $R_o$. The ductility factor $R_d$ represents the capability of the structure to dissipate the earthquake energy which is located in the range from 1.0 to 5.0. The overstrength factor $R_o$ indicates the reserve in the element capacity. It is located in the range from 1.0 to 1.7, and it defines the overstrength resulting from member size, the resistance factor considered in design, the material overstrength, the material strain hardening, and the unconsidered resistance that structure retains before a total failure occurs.

Generally, the response modification factor depends on two parameters which are overstrength and ductility. Overstrength is the additional unconsidered strength over the ultimate design strength that occurred in most structures. Material overstrength, strain hardening, and strength reduction factors are the main causes of the overstrength ($\Omega$):

$$\Omega = \frac{V_u}{V_d}, \tag{1}$$

where $V_u$ is the ultimate shear strength, $V_d$ is the design shear strength.

Ductility of a structure, or its members, is the ability to go through large inelastic deformations without major decrease of the strength or the stiffness. For the seismic loads, the ductility of the structure is an extremely important property. Newmark and Hall [21] state the ductility factor to be equal to the ratio between the ultimate deformation and the deformation at the initial yielding. They provided the following equations in order to define the ductility reduction factor ($R_\mu$):

Table 7: Parametric study results.

| Model | Strap brace thickness (mm) | $V_u$ (kN) | $V_y$ (kN) | $V_d$ (kN) | $\Delta_u$ (mm) | $\Delta_y$ (mm) | $\Omega$ | $R_\mu$ | $R$ | $R_y$ |
|---|---|---|---|---|---|---|---|---|---|---|
| Wall aspect ratio 1 : 1 (2.44 × 2.44), $F_y$ = 360 MPa | | | | | | | | | | |
| A1.5_36 | 1.5 | 65.5 | 49.2 | 36.9 | 165 | 14.3 | 1.78 | 4.70 | 8.34 | 2.2 |
| A2_36 | 2 | 82 | 64 | 48 | 155 | 16.5 | 1.71 | 4.22 | 7.21 | 1.65 |
| A2.5_36 | 2.5 | 99.3 | 78.6 | 58.95 | 138 | 18.5 | 1.68 | 3.73 | 6.28 | 1.35 |
| A3.0_36 | 3 | 114 | 93 | 69.75 | 104 | 20.5 | 1.63 | 3.02 | 4.94 | 1.1 |
| A3.5_36 | 3.5 | 125 | 104 | 78 | 36 | 21 | 1.60 | 1.56 | 2.50 | 0.95 |
| Wall aspect ratio 1 : 1 (2.44 × 2.44), $F_y$ = 230 MPa | | | | | | | | | | |
| A2.5_23 | 2.5 | 68.9 | 51.75 | 38.8125 | 115 | 12.2 | 1.78 | 4.23 | 7.50 | 1.9 |
| A3.0_23 | 3 | 79.6 | 60.8 | 45.6 | 101 | 13.4 | 1.75 | 3.75 | 6.55 | 1.55 |
| A3.5_23 | 3.5 | 87.6 | 68.9 | 51.675 | 85 | 14.5 | 1.70 | 3.27 | 5.55 | 1.37 |
| A4.0_23 | 4 | 96.4 | 77.6 | 58.2 | 58 | 15.6 | 1.66 | 2.54 | 4.20 | 1.2 |
| A4.5_23 | 4.5 | 101.4 | 83 | 62.25 | 25 | 16 | 1.63 | 1.46 | 2.37 | 1.05 |
| Wall aspect ratio 1 : 1 (1.20 × 2.44), $F_y$ = 360 MPa | | | | | | | | | | |
| B1.0_36 | 1 | 29.3 | 15.2 | 11.4 | 185 | 24 | 2.57 | 3.80 | 9.76 | 2.6 |
| B1.5_36 | 1.5 | 40.7 | 28.25 | 21.1875 | 210 | 26 | 1.92 | 3.89 | 7.48 | 1.75 |
| B2.0_36 | 2 | 49 | 30 | 22.5 | 130 | 26 | 2.18 | 3.00 | 6.53 | 1.3 |
| B2.5_36 | 2.5 | 54.8 | 36.5 | 27.375 | 118 | 31 | 2.00 | 2.57 | 5.15 | 1.05 |
| B3.0_36 | 3 | 55.6 | 39.12 | 29.34 | 58.9 | 31 | 1.90 | 1.67 | 3.17 | 0.9 |
| Wall aspect ratio 1 : 1 (1.20 × 2.44), $F_y$ = 230 MPa | | | | | | | | | | |
| B1.5_23 | 1.5 | 30.7 | 21 | 15.75 | 175 | 20 | 1.95 | 4.06 | 7.92 | 2.45 |
| B2.0_23 | 2 | 39.2 | 28.6 | 21.45 | 180 | 26 | 1.83 | 3.58 | 6.55 | 1.85 |
| B2.5_23 | 2.5 | 44.2 | 33.2 | 24.9 | 123 | 28 | 1.78 | 2.79 | 4.95 | 1.45 |
| B3.0_23 | 3 | 46.7 | 35.7 | 26.775 | 70 | 30 | 1.74 | 1.91 | 3.34 | 1.25 |

$V_u$ is the ultimate shear strength, $V_d$ is the design shear strength, $\Delta_u$ is the ultimate lateral displacement, $\Delta_y$ is the maximum elastic lateral displacement, $\Omega$ is the overstrength factor, and $R_\mu$ is the ductility factor. $R_y$ is the factor that overestimates the capacity of the brace according to AISI [23].

$$
\begin{aligned}
R_\mu &= 1.0 \quad (T < 0.03 \text{ second}),\\
R_\mu &= 2\mu - 1 \quad (1 > T > 0.03 \text{ second}),\\
R_\mu &= \mu \quad (T > 1.0 \text{ second}),\\
\mu &= \frac{\Delta u}{\Delta y},
\end{aligned}
\tag{2}
$$

where $\Delta_u$ is the ultimate lateral displacement and $\Delta_y$ is the maximum elastic lateral displacement. Knowing that the fundamental time periods for CFS framing buildings are located in the range between 0.1 and 0.5 s, the ductility factor $R_\mu$ can be presented as $R_\mu = 2\mu - 1$.

*5.1. Capacity Design Approach.* The capacity design approach is to design all the structural elements of the shear wall other than the strap brace using an amplified force. This amplified force is calculated by overestimating the strength capacity of the strap (system fuse) by two amplification factors $R_y$ and $R_t$. Values of $R_y$ and $R_t$ are listed for the Specially Concentrically Braced Frames (SCBF) in the Seismic Provisions for Structural Steel Buildings in AISC [22] and AISI S213 [8]. These factors are used in calculating the expected strength of the strap as follows:

$$
\begin{aligned}
T_n &= A_g \cdot R_y \cdot F_y,\\
T_u &= A_g \cdot R_t \cdot F_u.
\end{aligned}
\tag{3}
$$

After determination of $T_n$ and $T_u$, all other components in the shear wall (connections, studs, track, anchors, and hold-downs) should be designed to sustain the overexpected loads of the brace.

*5.2. The Parametric Study.* In order to study the response modification factor ($R$) for the CFS-braced shear walls, a parametric study is performed on 19 shear wall models using the previously verified FE model. Three main parameters are studied:

(i) The strap brace cross sectional area ($t$ = 1 to 4.5 mm)

(ii) The material yielding stress (2.3 and 3.6 MPa)

(iii) The wall aspect ratio (1 : 1 and 1 : 2)

The main objective of this study is to investigate the Response Modification Factor $R$ of different wall parameters and compare $R$ with $R_y$. $R_y$ factor defines the overestimating design value of all shear wall elements other than the brace by overestimating the brace strength. According to AISI [23], $R_y$ is taken 1.1 for material yielding stress 3.4 MPa or more while equalling 1.5 for material yielding stress 2.3 MPa.

Two wall models are studied with two different aspect ratios. The first wall model has dimensions of 2.44 m width and 2.44 m height. The studs of dimensions 152.4 × 41.3 × 12.7 × 1.5 mm, chord studs, are made of assembly of two studs back-to-back. The strap braces plate has 70 mm width and varying thickness. The second wall model has dimensions of 1.2 m width and 2.44 m height. The material is modeled as bilinear material with two different yield stress values. The first value is 360 MPa for $R_y$ 1.1. The second value is 230 MPa for $R_y$ 1.5. Figure 13 shows the walls' FE model. The parametric study results are listed in Table 7. Figure 14 shows $R$ versus $R_y$ factors for different wall aspect ratios and yield stresses.

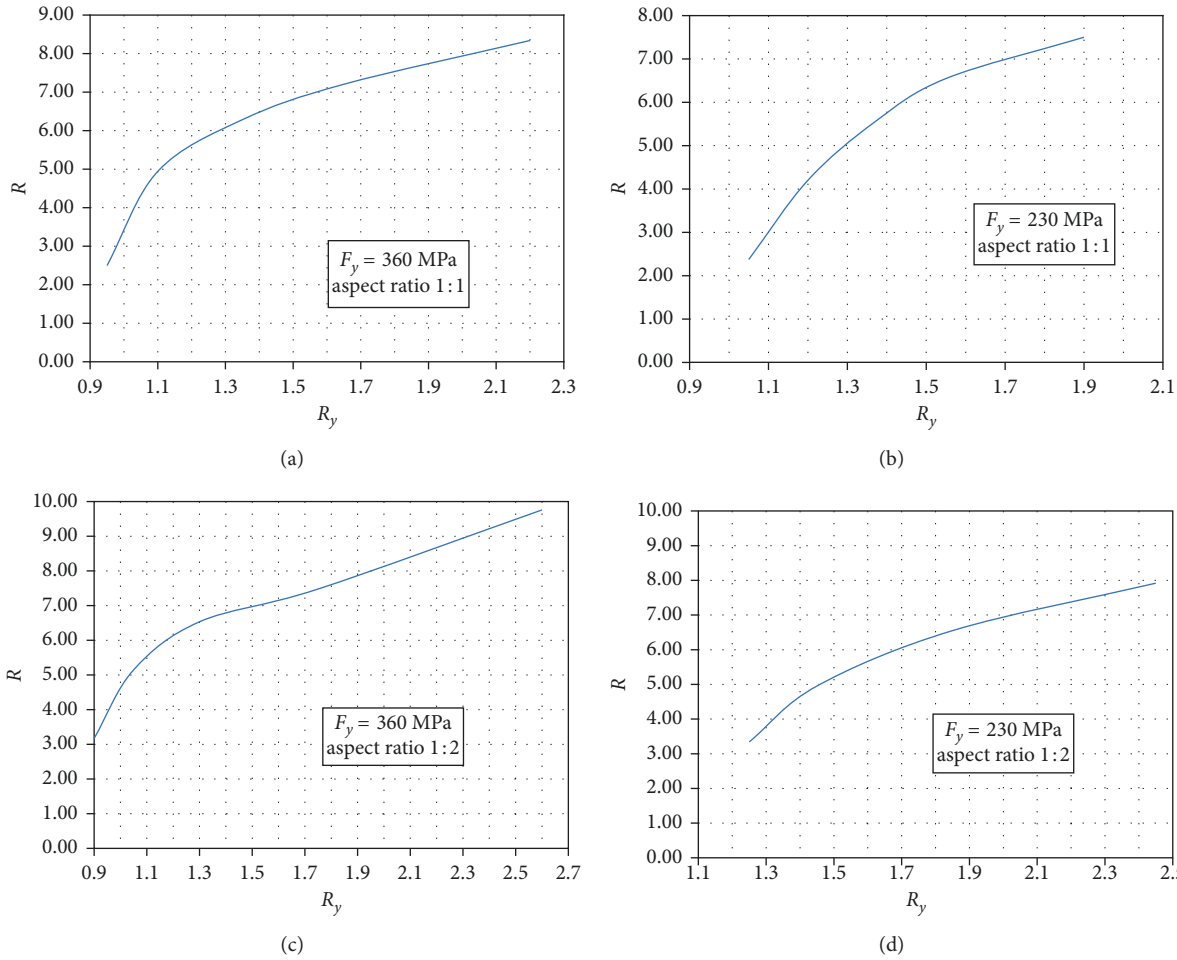


Figure 14: $R$ versus $R_y$ curves.

## 6. Results and Discussion

For each wall aspect ratio, yield stress, brace thickness, and $R_y$ factor, the Response Modification Factor $R$ is evaluated using the FE model. An eigen buckling analysis is performed to estimate the buckling length factor of the chord studs. This eigen buckling is performed first for hinged-hinged column with the same chord stud length. Another eigen buckling is performed to the chord stud in the wall assembly under compression. From the comparison of both eigen buckling loads, it is found that the buckling length factor $K$ for the chord stud is 0.5. This factor means that the gusset plates and the top track and the wall assembly give the studs rigid connections at ends.

For the same wall elements and varying strap brace thickness, different strap strengths to other wall elements strength ratios are calculated. These ratios define $R_y$ factor for the walls which results in different response modification factors $R$.

Results are listed in Table 7 and shown in Figure 10. It is clear that, for walls with aspect ratio 1 : 1 and yield stress 3.6 MPa, the $R$ factor is 5 at $R_y = 1.1$ which is greater than the value of 4 mentioned in specifications. For walls with yield stress 2.3 MPa, the $R$ factor is 6.2 at $R_y = 1.5$.

On the other hand, walls with aspect ratio equal 1 : 2 and yield stress 3.6 MPa have $R = 5.5$ at $R_y = 1.1$ which is greater than the value of 4 mentioned in American specifications. For walls with yield stress 2.3 MPa, the $R$ factor is 5.2 at $R_y = 1.5$ which is greater than the value of 4 mentioned in American specifications.

## 7. Conclusions

Based on the previous verification and parametric study, the following conclusions are reached:

(i) The ($R$) value considered by American specifications ASCE [18] is conservative.

(ii) Using weak brace with sufficient ductility and on the other side having strong connections, chord studs, and reinforced track and applying the capacity design approach, the $R$ factor can be increased to 4.5 or even 5 for walls with aspect ratio 1 : 1 and 1 : 2.

(iii) The finite element method gives an accurate simulation for the strap-braced shear walls in both elastic and inelastic ranges. It considers different material and geometric nonlinearities and accurately simulates the real behavior of the hold-downs.

## Conflicts of Interest

The authors declare that they have no conflicts of interest.

## References


[1] C. M. Uang, "Establishing $R$ (or $R_w$) and $C_d$ factors for building seismic provisions," *Journal of Structural Engineering*, vol. 117, no. 1, pp. 19–28, 1991.

[2] M. Al-Kharat and C. A. Rogers, "Inelastic performance of screw connected light gauge steel strap braced walls," Research Report, Department of Civil Engineering & Applied Mechanics, McGill University, Montreal, QC, Canada, 2006.

[3] M. Al-Kharat and C. A. Rogers, "Inelastic performance of cold-formed steel strap braced walls," *Journal of Constructional Steel Research*, vol. 63, no. 4, pp. 460–474, 2007.

[4] M. Al-Kharat and C. A. Rogers, "Inelastic performance of screw connected cold-formed steel strap braced walls," *Canadian Journal of Civil Engineering*, vol. 35, no. 1, pp. 11–26, 2008.

[5] M. Casafont, A. Arnedo, F. Roure, and A. Rodríguez-Ferran, "Experimental testing of joints for seismic design of lightweight structures Part 1. Screwed joints in straps," *Thin-Walled Structures*, vol. 44, no. 2, pp. 197–210, 2006.

[6] S. Hatami, H. R. Ronagh, and M. Azhari, "Behaviour of thin strap-braced cold-formed steel frames under cyclic loads," in *Proceedings of the Fifth International Conference on Thin-Walled Structures*, vol. 1, pp. 363–370, Brisbane, Australia, June 2008.

[7] K. Velchev, G. Comeau, N. Balh, and C. A. Rogers, "Evaluation of the AISI S213 seismic design procedures through testing of strap braced cold-formed steel walls," *Thin-Walled Structures*, vol. 48, no. 10, pp. 846–856, 2010.

[8] AISI American Iron and Steel Institute, *North American Standard for Cold-Formed Steel Framing—Lateral Design-S213*, AISI, Washington, DC, USA, 2007.

[9] M. Mahmoudi and M. G. Abdi, "Evaluating response modification factors of TADAS frames," *Journal of Constructional Steel Research*, vol. 71, pp. 162–170, 2012.

[10] M. Abu-Hamd and B. El-Samman, "Buckling strength of axially loaded cold formed built-up I-sections," in *Proceedings of the Annual Stability Conference-Structural Stability Research Council*, St. Louis, MO, USA, April 2013.

[11] R. Landolfo, O. Iuorio, V. Macillo, M. T. Terracciano, T. Pali, and L. Fiorino, "Seismic response of Cfs strap-braced stud walls: experimental investigation," *Thin-Walled Structures*, vol. 85, pp. 466–480, 2014.

[12] ANSYS, *ANSYS 14.5*, ANSYS Inc., Canonsburg, PA, USA, 2012.

[13] S. G. Buonopane, T. H. Tun, and B. W. Schafer, "Fastener-based computational models for prediction of seismic behavior of CFS shear walls," in *Proceedings of the 10th US National Conference on Earthquake*, Anchorage, AK, USA, July 2014.

[14] J. Leng, B. W. Schafer, and S. G. Buonopane, "Modeling the seismic response of cold-formed steel framed buildings: model development for the CFS-NEES building," in *Proceedings of the Annual Stability Conference-Structural Stability Research Council*, St. Louis, MO, USA, April 2013.

[15] R. Serrette and D. Peyton, "Strength of screw connections in cold-formed steel construction," *Journal of Structural Engineering*, vol. 135, no. 8, pp. 951–958, 2009.

[16] S. M. W. Corner, "Screw-fastened cold-formed steel-to-steel shear connection behavior and models," M.Sc. thesis, Virginia Polytechnic Institute and State University, Blacksburg, VA, USA, 2014.

[17] V. Zeinoddini and B. W. Schafer, "Simulation of geometric imperfections in cold-formed steel members," in *Proceedings of the Annual Stability Conference, Structural Stability Research Council, SSRC*, Grapevine, TX, USA, April 2012.

[18] ASCE-07 American Society of Civil Engineers, *Minimum Design Loads for Buildings and Other Structures*, ASCE, Irvine, CA, USA, 2010.

[19] US Army Corps of Engineers, *Technical Instructions: Design of Cold-Formed Load Bearing Steel Systems and Masonry Veneer/Steel Stud Walls*, Ti 809-07, Engineering and Construction Division, Directorate of Civil Works, Washington, DC, USA, 2003.

[20] NRCC, *National Building Code of Canada*, National Research Council of Canada, Ottawa, ON, Canada, 2005.

[21] N. M. Newmark and W. J. Hall, *Earthquake Spectra and Design, Engineering Monograph MNO-3*, Earthquake Engineering Research Institute, Berkeley, CA, USA, 1982.

[22] AISC American Institute of Steel Construction, *Design Specifications*, AISC, Chicago, IL, USA, 2010.

[23] AISI American Iron and Steel Institute, *North American Specification for the Design of Cold Formed Steel Structural Members*, AISI, Washington, DC, USA, 2007.